

# Symmetry-Breaking Motility

Allen Lee,<sup>1</sup> Ha Youn Lee,<sup>1,2</sup> and Mehran Kardar<sup>1</sup>

<sup>1</sup>*Department of Physics, Massachusetts Institute of Technology, Cambridge, Massachusetts 02139*

<sup>2</sup>*Department of Physics, The Ohio State University, Columbus, Ohio 43210*

(Dated: July 29, 2004)

Locomotion of bacteria by actin polymerization, and *in vitro* motion of spherical beads coated with a protein catalyzing polymerization, are examples of active motility. Starting from a simple model of forces locally normal to the surface of a bead, we construct a phenomenological equation for its motion. The singularities at a continuous transition between moving and stationary beads are shown to be related to the symmetries of its shape. Universal features of the phase behavior are calculated analytically and confirmed by simulations. Fluctuations in velocity are shown to be generically non-Maxwellian and correlated to the shape of the bead.

Motility, the capacity of organisms for independent motion, has long fascinated physicists as well as biologists. For example, the reversible character of low Reynolds number flows [1] requires ingenious methods for swimming motion [2]. Another strategy for movement, the subject of this paper, is propulsion via forces generated by polymerization of actin on an organism's surface. Polymerizing actin filaments are involved in, among other things, the locomotion of certain bacteria, such as the pathogenic *Listeria monocytogenes*. Upon entering the cytoplasm of a host, a *Listeria* "hijacks" the cell's actin machinery; first a roughly symmetrical cloud of polymerizing actin filaments envelops the bacterium, and then an asymmetric "comet tail" of actin spontaneously develops that propels the bacterium forward [3]. Motility by actin polymerization has been the subject of several analytical and model studies [4–8].

A number of *in vitro* experiments have been performed on artificial systems designed to mimic *Listeria* motility under simplified and more easily controlled circumstances [9–13]. In these experiments, the bacteria are replaced with spherical beads coated with a protein that catalyzes actin polymerization. When these functionalized beads are placed in cell extracts or a mixture of purified proteins, phenomenology similar to that of *Listeria* motility is observed. A spherically symmetric cloud of cross-linked actin filaments forms around each bead. Then, depending on the various parameters of the experiment, some beads are observed to spontaneously break free of their actin clouds and move away, propelled by an asymmetric actin comet tail.

Several theories have been put forward to explain the mechanism behind this spontaneous motility. van Oudenaarden and Theriot model the actin filaments surrounding the bead as elastic Brownian ratchets [14]. The stochastic growth of these filaments is coupled due to the presence of the bead; when one filament grows, it gives the bead a small push, making room for neighboring filaments to grow. This cooperativity generates positive feedback and the possibility of an avalanching symmetry-breaking event. In another model, Noireaux et al have proposed that the actin cloud surrounding the bead be

treated as an elastic gel [15]. Polymerization occurs at the bead surface, which expands the gel and stretches it. At a certain point, stress at the outer surface ruptures the gel, and the bead is free to escape. Mogilner and Oster have suggested a third alternative in which movement occurs because of the failure of cross-links within the actin network [8].

Our aim is not to reconcile these existing theories, or to provide a comprehensive description of the observed phenomena. Instead, we investigate the behavior of an *activated rigid bead* within a framework that is sufficiently general to include many possible microscopic models. In the spirit of the Landau theory of magnetism, we treat the actin filaments surrounding the bead as a continuous effective field that generates a normal force density at each point on the bead surface. The evolution of this order parameter field is coupled to the velocity of the bead, allowing the possibility of positive feedback as in the above Brownian ratchet model [14]. Our approach neglects many aspects of the system, but can provide answers regarding generic features: What are the possible singularities that can accompany the transition between stationary and moving states, and how do they depend on the shape of the bead? Regarding the active bead as a stochastic system, are there characteristics of its fluctuations that set it apart from a passive (Brownian) bead?

We consider a bead of fixed shape, with unit normal vector  $\hat{\mathbf{n}}(\mathbf{r})$  at a point  $\mathbf{r}$  on its surface. The polymerization of actin (or any other actively energy-consuming process for that matter) is assumed to exert a force, locally directed along the normal, at each point on the bead surface. The force per unit area at time  $t$  is indicated by a scalar field  $g(\mathbf{r}, t)$ , which could for example be a function of the actin density at that point. The net force due to such activity, acting on the center of mass of the bead, is  $\mathbf{F}_a(t) \equiv \int dS g(\mathbf{r}, t) \hat{\mathbf{n}}(\mathbf{r})$ , the integration being over the entire bead surface. In response to force, the bead moves at an instantaneous velocity  $\mathbf{v}(t)$ . In a viscous medium the components of the force and velocity are linearly related by  $v_\alpha = \mu_{\alpha\beta} F_\beta$  with  $\alpha, \beta = 1, 2, 3$ , where the mobility tensor  $\mu_{\alpha\beta}$  depends on the shape of the object. For functionalized beads propelled by a comet tail,

drag from tethered filaments in fact far exceeds viscous drag [11]. Whether this would be true for a stationary bead in an actin cloud is unknown. However, we are relatively unconcerned about the exact nature of the drag force: For small enough velocities, it should be possible to make a linear expansion in force, with higher-order corrections appearing at higher speeds.

To complete the description of the dynamics, we need to specify the time evolution of  $g$ . We assume that the rate of change of  $g(\mathbf{r}, t)$  is a *local* function of  $g$ , and that it depends on the net velocity  $\mathbf{v}$ . The dependence on  $\mathbf{v}$  couples the field  $g$  at different positions on the bead and also provides the possibility of positive feedback (e.g. when polymerization is decreased on the front, and enhanced on the rear of a moving bead). The growth rate is then expanded in powers of  $g$  and  $\mathbf{v}$ , resulting in

$$\frac{\partial g(\mathbf{r}, t)}{\partial t} = \Phi[g(\mathbf{r}), \mathbf{v}] = -g + a\mathbf{v} \cdot \hat{\mathbf{n}} - g^2 + bg\mathbf{v} \cdot \hat{\mathbf{n}} + d\mathbf{v} \cdot \mathbf{v} + e(\mathbf{v} \cdot \hat{\mathbf{n}})^2 - cg^3 + \dots + \eta(\mathbf{r}, t), \quad (1)$$

where we have included all terms to second order, and the simplest cubic term. Note that the vector  $\mathbf{v}$  contributes through scalar forms  $v_\perp = \mathbf{v} \cdot \hat{\mathbf{n}}$  and  $v^2 = \mathbf{v} \cdot \mathbf{v}$ . Such an expansion is presumably valid close to a continuous transition in which both  $g$  and  $\mathbf{v}$  are small, and needs to be self-consistently justified. We have rescaled  $g$  and  $t$  so that the coefficients of  $g$  and  $g^2$  are both  $-1$ . The sign of the linear term is negative so that a uniform actin distribution (set to  $g = 0$  without loss of generality) is stable in the absence of any velocity coupling, while the sign of the  $g^2$  term is unimportant since we may always consider the dynamics of  $-g$  rather than  $g$ . In addition to rescaling  $g$  and  $t$ , we may also rescale lengths; a convenient choice is to set the surface area of the bead to unity. Through appropriate redefinitions, our previous formulas for the force  $\mathbf{F}_a(t)$  and bead velocity  $\mathbf{v}$  remain unchanged. For analysis and numerical simulations of Eq. (1) we typically set  $d = e = \dots = 0$ , and  $c > 0$  for stability. The final term in Eq. (1) allows for a stochastic noise  $\eta(\mathbf{r}, t)$ .

In the absence of an external force, Eq. (1), along with the formula for velocity

$$v_\alpha(t) = \mu_{\alpha\beta} F_\beta(t) = \mu_{\alpha\beta} \int dS g(\mathbf{r}, t) n_\beta(\mathbf{r}), \quad (2)$$

fully specifies our model. We first analyze the case of a spherical bead, and then generalize its lessons to more complicated shapes. Due to its symmetry, the velocity and force are parallel for a sphere, and  $\mu_{\alpha\beta} = \mu\delta_{\alpha\beta}$ . In the absence of noise  $\eta$ , there is a trivial solution of  $g(\mathbf{r}, t) = \mathbf{v}(t) = 0$ , which corresponds to a static, uniform actin distribution and a motionless bead. This solution is linearly stable for  $a < 3/\mu$ , but unstable to dipolar fluctuations for  $a > 3/\mu$ . In the latter case, the unstable actin fluctuations grow and saturate. Thus Eq. (1)

allows for a symmetry-breaking transition from a bead at rest ( $\mathbf{v} = 0$ ) to a bead in motion ( $\mathbf{v} = \text{const}$ ) as the parameter  $a$  is varied past a critical value  $a_c = 3/\mu$ . This parameter controls the strength of the positive feedback in the coupling of the bead velocity to the actin field.

Near this transition we expand  $g$  in spherical harmonics with  $g(\mathbf{r}, t) \rightarrow g(\Omega, t) = \sum_{\ell m} g_{\ell m}(t) Y_{\ell m}(\Omega)$ , where  $\Omega$  represents the solid angle coordinates  $\theta$  and  $\phi$ . In this basis Eq. (1) becomes

$$\frac{dg_{\ell m}}{dt} = \left(-1 + \frac{\mu a}{3} \delta_{\ell 1}\right) g_{\ell m} + \text{nonlinear terms}, \quad (3)$$

where the nonlinear terms couple different  $g_{\ell m}$ 's with coefficients of the form  $\int d\Omega Y_{\ell_1 m_1} Y_{\ell_2 m_2} Y_{\ell_3 m_3}^* Y_{\ell_4 m_4}^*$ ,  $\dots$ . From the linear terms in Eq. (3) we see that, near the transition with  $\epsilon \equiv \mu(a - a_c)/3$ ,  $|\epsilon| \ll 1$  and for small actin fluctuations, the dipolar ( $\ell = 1$ ) modes evolve on a slow time scale  $t \propto \epsilon^{-1}$ , while the other modes evolve on a fast time scale  $t \propto \mathcal{O}(1)$ . Due to their instability (or near instability) we also expect the dipolar modes to be larger than the others. We therefore treat the fast  $\ell \neq 1$  modes as adiabatically slaved to the slow  $\ell = 1$  modes and self-consistently solve for their amplitudes as functions of the  $g_{1m}$ 's. Substitution then yields effective equations of motion for the slow modes, and by a simple transformation, the bead velocity [20], as

$$\frac{d\mathbf{v}}{dt} = \epsilon \mathbf{v} + \frac{27}{5\mu^2} \left[ \left( \frac{\mu b}{3} - 1 \right) \left( \frac{\mu b}{3} - 2 \right) - c \right] \mathbf{v}^3 + u \mathbf{v}^5 + \dots, \quad (4)$$

with  $\mathbf{v}^3 \equiv v^2 \mathbf{v}$ , etc. Thus, near the transition the bead velocity  $\mathbf{v}$  obeys a Ginzburg-Landau equation consistent with spherical symmetry. When the coefficient of the cubic term is negative, the transition to nonzero  $\mathbf{v}$  is continuous with the steady state velocity  $\mathbf{v}^*$  going to zero as  $\epsilon \rightarrow 0^+$ . In the vicinity of this continuous transition in parameter space, our analysis above is self-consistently justified and Eq. (4) should provide an accurate description of the dynamics. The fifth-order coefficient  $u$ , although not explicitly presented above, is negative in this region, providing overall stability.

The phase diagram and critical behavior associated with the steady-state solutions  $\mathbf{v}^*$  of Eq. (4) are familiar from mean-field theory in equilibrium statistical mechanics. The cubic coefficient is negative when  $b_{c1} < b < b_{c2}$ , where  $b_{c1}$  and  $b_{c2}$  are the two roots of  $(\mu b/3 - 1)(\mu b/3 - 2) = c$  (recall that  $c > 0$ ). In this regime, the transition is continuous with  $\mathbf{v}^* \propto \epsilon^{1/2}$ . When the cubic coefficient is positive, the transition is discontinuous. Tricritical points, at which  $\mathbf{v}^* \propto \epsilon^{1/4}$ , occur when  $b = b_{c1}$  or  $b = b_{c2}$  precisely. Along the line  $a = a_c$  or  $\epsilon = 0$ ,  $\mathbf{v}^* \propto |b - b_{ci}|^{1/2}$  for  $i = 1, 2$  as  $b$  varies outside of the interval  $[b_{c1}, b_{c2}]$ . Finally, in the vicinity of the first-order transition with  $b > b_{c2}$  or  $b < b_{c1}$ , the  $\mathbf{v} = 0$  and  $\mathbf{v} = \text{const}$  states coexist, both being locally

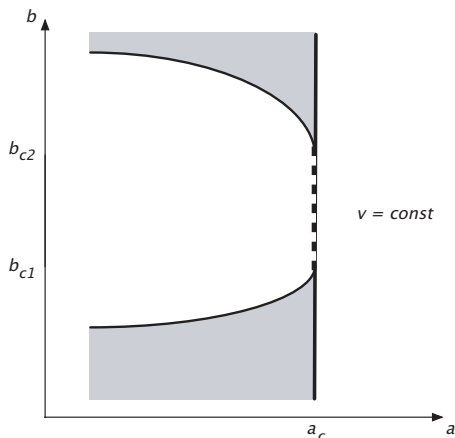


FIG. 1: Schematic phase diagram for a spherical bead in the vicinity of continuous transitions for  $a = a_c$  and  $b_{c1} < b < b_{c2}$ . In the grey region both stationary ( $\mathbf{v} = 0$ ) and moving ( $\mathbf{v} = \text{const}$ ) states are locally stable.

stable. In the  $a$ -direction, this region extends over the range  $a^* < a < a_c$  where the “limit of metastability”  $a^*$  has the  $b$  dependence  $a_c - a^* \propto (b - b_c)^2$  for  $b < b_{c1}$  or  $b > b_{c2}$ . The schematic phase diagram for the motion of the bead is shown in Fig. 1.

To confirm the analytical results, we numerically simulated Eq. (1) with a fourth-order Runge-Kutta scheme. For integrations over the surface of the spherical bead, we adapted routines from the NAG library [16]. We confirmed the phase diagram in Fig. 1, as well as the various critical exponents. As an example of the latter, Fig. 2 illustrates the time evolution of velocity for  $a > a_c = 1$ . Starting from an initial (unstable) stationary state, any small fluctuation takes the sphere into a moving phase. The characteristic time scale for this change of state diverges as  $\epsilon^{-1} \propto 1/(a - a_c)$ , while the saturation velocity scales as  $\epsilon^{1/2} \propto \sqrt{a - a_c}$ . As indicated in Fig. 2, the velocity evolution curves obtained for a number of different  $a$  can be collapsed together using the above scalings of velocity and time.

Let us now consider a rigid bead of arbitrary shape. The acceleration of the bead can be obtained by taking a time derivative of Eq. (2) and substituting from Eq. (1). The analog of Eq. (4) for the sphere is then obtained as

$$\frac{dv_\alpha}{dt} = (-\delta_{\alpha\beta} + a \mu_{\alpha\gamma} \overline{n_\gamma n_\beta}) v_\beta + \dots + f_\alpha(t). \quad (5)$$

At the linear order, properties of the shape are encoded in the tensor  $\overline{n_\alpha n_\beta} \equiv \int dS n_\alpha(\mathbf{r}) n_\beta(\mathbf{r})$ . The stochastic force  $f_\alpha(t)$  partly originates in the noise in Eq. (1), and correlations amongst its components also depend on the shape through the matrices  $\mu_{\alpha\beta}$  and  $\overline{n_\alpha n_\beta}$ . The linear

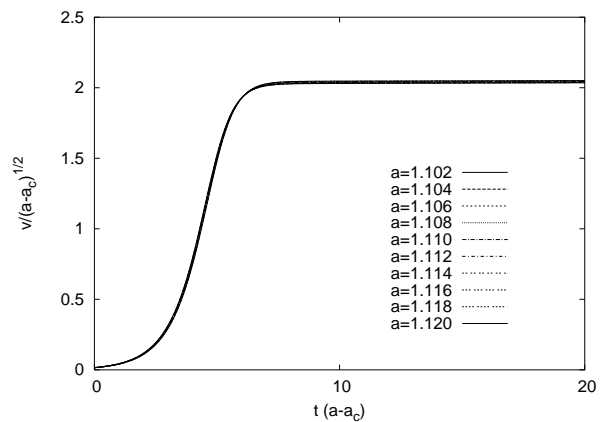


FIG. 2: Rescaled bead speed versus rescaled time for  $\mu = 3$ ,  $c = 0.2$ ,  $b = 1.5$  ( $b_{c1} \approx 0.83$  and  $b_{c2} \approx 2.17$ ), and various values of  $a > a_c = 1$ . The bead begins (very nearly) at rest at  $t = 0$  with a small random actin distribution. The curves are nearly perfectly superimposed.

stability of a stationary bead is determined by the eigenvalues  $\{\lambda_i\}$  of the matrix  $\boldsymbol{\mu} \cdot \overline{\mathbf{n}\mathbf{n}}$ . When  $a\lambda_i > 1$ , the bead is unstable to motion in the corresponding eigendirection. The largest eigenvalue indicates the direction that initially becomes unstable. Of course, as in Fig. 1, it is possible to have coexistence of moving and stationary states before the onset of this instability. In fact, the analysis so far does not rule out coexistence of several states moving along different directions [21].

It is interesting to note that eigenvalues of  $\overline{\mathbf{n}\mathbf{n}}$  are larger along directions where the shape displays a bigger cross-section. Thus, ignoring variations in mobility, a pancake shape prefers to move along its axis (breaking a two-fold symmetry), while a cigar shape moves perpendicular to the axis (breaking a degeneracy in angle). This is opposite to what happens for passive ellipsoids in a fluid where hydrodynamic effects favor motion along the slender axis.

To see what happens when the stationary bead is linearly unstable, we need to examine the higher-order terms in Eq. (5) [22]. *If the transition is continuous*, its singularities are determined by the next higher-order term in the expansion. For the sphere, symmetry considerations rule out a quadratic term; the cubic term leads to the singularities discussed earlier. However, quadratic terms  $v_\beta v_\gamma$  may appear in Eq. (5) with coefficients  $C_{\alpha\beta\gamma}$  that are related to the shape by  $\overline{n_\alpha n_\beta n_\gamma} \equiv \int dS n_\alpha(\mathbf{r}) n_\beta(\mathbf{r}) n_\gamma(\mathbf{r})$ . If such terms are present, the velocity will vanish on approaching the transition as  $\epsilon$ , rather than  $\sqrt{\epsilon}$ . To distinguish the two universality classes along a particular direction, we merely need to ask if the opposite direction is equivalent. Thus the velocity of a cigar-shape will vanish as  $\sqrt{\epsilon}$ , while that of an arrowhead goes to zero linearly. In the language of dynamical systems, the transition at  $\epsilon = 0$  is a pitchfork

bifurcation in the former case and a transcritical bifurcation in the latter [17].

Let us now consider the effect of the noise  $f_\alpha(t)$  in Eq. (5). At a coarse level this resembles a Langevin equation for the velocity  $\mathbf{v}$ . However, since this dynamic equation is not subject to fluctuation–dissipation constraints, the resulting probability distributions need not be those familiar from equilibrium statistical physics. For example, let us consider an ellipsoidal shape in the regime where stationary motion is stable, and higher-order terms in Eq. (5) can be ignored. For a passive (Brownian) ellipsoid, the velocity fluctuations follow a Maxwell probability distribution. In this case the center of mass velocity is equally likely to point in any direction, irrespective of the orientation of the ellipsoid. For active fluctuations (e.g. due to actin polymerization) of the same bead, the probability distribution of velocities can be extracted from Eq. (5). Linear truncation leads to a Gaussian probability distribution,  $P(\mathbf{v}) \propto \exp(-v_\alpha M_{\alpha\beta} v_\beta)$ , but there is no a priori reason for the matrix  $M_{\alpha\beta}$  to be proportional to  $\delta_{\alpha\beta}$ . Thus generically the velocity fluctuations of the active bead are non-Maxwellian, and correlated with the shape of the bead.

In summary, motivated by experiments on actin-based motility, we have characterized some of the phenomena that distinguish such an active system from a passive Brownian particle. We start with a highly simplified microscopic model whose central ingredients are a force that is (a) locally normal to the surface of a rigid bead, and (b) influenced by the velocity of the bead in the surrounding medium. These assumptions lead to a macroscopic equation for the bead velocity whose coefficients reflect the symmetries in its shape. (The reliance on symmetry should increase the validity of the form of this equation beyond our particular microscopic model.) We note that Eq. (1) for the dynamics of the actin distribution is similar to equations that model pattern formation [18] or “self-organization” [19] in various contexts. As in our case, analysis of these systems near threshold can often be performed by eliminating fast modes.

With the macroscopic equation for the bead velocity we can analyze the singularities that accompany a continuous transition between stationary and moving states. Depending on symmetries along the direction of movement, the velocity vanishes with a square-root or linear singularity. We also examined the fluctuations in velocity of an active bead. We find that, generically, the probability distribution is not Maxwellian in form, and is dependent upon the orientation of the bead. It would be interesting to experimentally determine this distribution through single-molecule experiments on active beads. In this work we focused only on the translational motion of a freely moving bead. Rotations of a bead, as well as its motion in a trap, are likely to bring in additional degrees of freedom (position and angular coordinates) that are coupled to the velocity of the bead. In future work,

we would like to incorporate such effects to form a more complete picture of the repertoire of motions available to active beads.

The authors thank Arpita Upadhyaya for helpful discussions, and acknowledge support from the NSF grant DMR-01-18213 (MK), a University Postdoctoral Fellowship from The Ohio State University (HYL), and an NSF Graduate Fellowship (AL).

- 
- [1] E. M. Purcell, Am. J. of Phys. **45**, 3 (1977).
  - [2] A. Najafi and R. Golestanian, Phys. Rev. E **69**, 062901/1 (2004).
  - [3] L. G. Tilney and D. A. Portnoy, J. Cell. Biol. **109**, 1597 (1989).
  - [4] C. Peskin, G. Odell, and G. Oster, Biophys. J. **65**, 316 (1993).
  - [5] A. Mogilner and G. Oster, Biophys. J. **71**, 3030 (1996).
  - [6] F. Gerbal, P. Chaikin, Y. Rabin, and J. Prost, Biophys. J. **79**, 2259 (2000).
  - [7] A. E. Carlsson, Biophys. J. **81**, 1907 (2001).
  - [8] A. Mogilner and G. Oster, Biophys. J. **84**, 1591 (2003).
  - [9] D. Yarar, W. To, A. Abo, and M. D. Welch, Curr. Biol. **9**, 555 (1999).
  - [10] A. B. Groswasser, S. Wiesner, R. M. Golsteyn, M. F. Carlier, and C. Sykes, Nature **417**, 308 (2002).
  - [11] S. Wiesner, E. Helfer, D. Didry, G. Ducouret, F. Lafuma, M. F. Carlier, and D. Pantaloni, J. Cell. Biol. **160**, 387 (2003).
  - [12] S. Samarin, S. Romero, C. Kocks, D. Didry, D. Pantaloni, and M. F. Carlier, J. Cell. Biol. **163**, 131 (2003).
  - [13] L. Cameron, M. J. Footer, A. van Oudenaarden, and J. A. Theriot, Proc. Natl. Acad. Sci. U.S.A. **96**, 4908 (1999).
  - [14] A. van Oudenaarden and J. A. Theriot, Nature Cell Biol. **1**, 493 (1999).
  - [15] V. Noireaux, R. M. Golsteyn, E. Friederich, J. Prost, C. Antony, D. Louvard, and C. Sykes, Biophys. J. **78**, 1643 (2000).
  - [16] URL <http://www.nag.com/numeric/fl/manual/html/FLlibrarymanual.asp>.
  - [17] S. Strogatz, *Nonlinear Dynamics and Chaos* (Addison Wesley, Reading, MA, 1994).
  - [18] M. C. Cross and P. C. Hohenberg, Rev. Mod. Phys. **65**, 851 (1993).
  - [19] H. Haken, *Synergetics* (Springer-Verlag, Berlin, 1983).
  - [20] Equation (4) neglects terms of the form  $\epsilon^n \mathbf{v}^3$  with  $n = 1, 2, 3, \dots$  and similarly at order  $\mathbf{v}^5$ . Calculation of these terms by adiabatic elimination requires more care.
  - [21] Throughout the paper we assume a uniform coating of the bead. This assures the absence of a constant term in Eq. (5) since  $\int dS n_\alpha(\mathbf{r}) = 0$  for any closed surface.
  - [22] To consider Eq. (5) beyond linear order, we adiabatically eliminate all modes of  $g(\mathbf{r}, t)$  except the three-dimensional subspace corresponding to  $\{v_\alpha\}$ . This is only reasonable near the transition when  $|a\lambda_1 - 1| \ll 1$ , where  $\lambda_1$  is the largest eigenvalue of  $\boldsymbol{\mu} \cdot \overline{\mathbf{n}\mathbf{n}}$ . The elimination of fast modes is only partial, in that the components of  $\mathbf{v}$  in directions perpendicular to the unstable eigenvector are fast, but still retained.